Aqueous Microsolvation of Mercury Halide Species†

Benjamin C. Shepler, Ashby D. Wright, Nikolai B. Balabanov, and Kirk A. Peterson*

Department of Chemistry, Washington State University, Pullman, Washington 99164-4630

Received: March 15, 2007; In Final Form: May 3, 2007

The effects of aqueous solvation on the thermochemistry of reactions between mercury and small halogen molecules has been investigated by the microsolvation approach using ab initio and density functional theory (DFT) calculations. The structures, vibrational frequencies, and binding energies of 1, 2, and 3 water molecules with mercury-halide ($HgBr_2$, HgBrCl, $HgCl_2$, HgBr, and HgCl) and related mercury and halogen species (Br_2, BrCl, Cl_2, Cl, Hg, and Br) have been computed with second order Møller−Plesset perturbation theory (MP2) and the B3LYP density functional method. Accurate incremental water binding energies have been obtained at the complete basis set (CBS) limit using sequences of correlation consistent basis sets, including higher order correlation effects estimated from coupled cluster calculations. The resulting energetics were used to calculate the influence of water molecules on the thermochemistry of a number of reactions between mercury and small halogen-containing molecules. In general, the presence of water favors the formation of oxidized mercury halide species.

I. Introduction

Unusual behavior has recently been observed in the polar tropospheric chemistry of mercury. Throughout the dark winter months, the concentration of mercury in the polar troposphere remains near its global background concentration of 1−2 ng/m^3.[1] However, following polar sunrise, the mercury concentration fluctuates drastically and tends toward lower concentrations, often dropping as low as 0.1 ng/m^3.[2−6] These fluctuations, which have been called mercury depletion events (MDEs), closely resemble ozone depletion events that are known to be caused by reactions with small reactive halogen species such as Br and BrO.[7−11] This has led to the proposal that the MDEs are a result of the oxidation of gaseous elemental mercury (the dominant form of mercury in the atmosphere) by reactions with the same halogen species.[2−5,12−14] These oxidized mercury species are then thought to be deposited on the snowpack.[3,13,14] This hypothesis has led to numerous experimental[15,16] and theoretical[17−25] studies on the gas-phase kinetics and thermochemistry of possible mercury−halogen reactions that may be involved. In addition to gas-phase reactions, it is likely that water plays an important role in MDEs. The deposition of the oxidized mercury species on snow and ice surfaces obviously involves water. It is also possible that clouds, water droplets, and ice surfaces may catalyze the mercury oxidation process.[14]

Because of the potential importance of water in MDEs, an ab initio study has been carried out to investigate the effects of aqueous solvation on a number of mercury- and halogen-containing species. Those that have been studied are $HgBr_2$, $HgCl_2$, HgBrCl, HgBr, HgCl, Br_2, Cl_2, BrCl, Hg atom, Br atom, and Cl atom. The binding energies and structures of these species with one, two, and three water molecules have been determined. The effects on the gas-phase thermochemistry due to these numbers of water molecules have also been examined for the following reactions:

Atom−Atom Recombination

$$Hg + X \rightarrow HgX \ (X = Br, Cl) \quad (1)$$

Atom−Diatom Recombination

$$HgX + Y \rightarrow HgXY \ (X, Y = Br, Cl) \quad (2)$$

Abstraction

$$HgX + Y \rightarrow Hg + XY \ (X, Y = Br, Cl) \quad (3)$$

Insertion

$$Hg + XY \rightarrow HgXY \ (X, Y = Br, Cl) \quad (4)$$

The interaction of the Hg atom with a single water molecule has been reported previously,[26] but the microsolvation of the other mercury species in this study have not previously appeared in the literature. There have been a number of previous investigations, however, into water complexes involving halogen atoms[27−29] and diatomic halogen molecules.[30−37]

II. Methodology

Geometry optimizations were carried out for 11 species ($HgBr_2$, $HgCl_2$, HgBrCl, HgBr, HgCl, Br_2, Cl_2, BrCl, Hg, Br, and Cl) with one, two, and three water molecules. For each complex, the optimizations employed second order Møller−Plesset perturbation theory (MP2).[38] For the open shell molecules, unrestricted Hatree-Fock (UHF) calculations were used to determine the reference wave functions, and the unrestricted MP2 method (UMP2) was used for the electron correlation. In all calculations, the frozen-core approximation was employed, and in these cases, the Br 3d electrons were included in the core. The basis sets used throughout this work corresponded to cc-pV*n*Z-PP for Hg[39] and Br,[40] and aug-cc-pV*n*Z[41,42] for H, O, and Cl (n = D, T, Q). In the cases of the weakly bound Hg + $(H_2O)_m$ complexes, however, diffuse-augmented basis sets (aug-cc-pV*n*Z-PP) were also used on Hg. In any event, these basis set combinations will henceforth be denoted by simply aVDZ, aVTZ, and aVQZ for n = D, T, and Q, respectively. It should be noted that the use of an aug-cc-pVDZ-PP basis set on Hg

† Part of the "Thom H. Dunning, Jr., Festschrift".

10.1021/jp072093d CCC: $37.00
Published on Web 06/27/2007

was tested for the $HgBr_2-(H_2O)_2$ complex at the MP2 level of theory. The resulting counterpoise corrected binding energy (see below) was within 0.01 kcal/mol of the value calculated without the additional diffuse functions on Hg. Energy consistent relativistic pseudopotentials (PPs) of the Stuttgart−Köln variety were used on the Hg[43] and Br[40] atoms. The Hg PP leaves the $5s^25p^65d^{10}6s^2$ electrons to be explicitly treated, and the Br PP replaces all but the $3s^23p^63d^{10}4s^24p^5$ electrons. The aVDZ basis sets were used in the geometry optimizations. Geometries were also optimized with the B3LYP[44,45] hybrid density functional method, again employing the aVDZ basis sets. However, the latter calculations did not include the Hg-atom complexes because the B3LYP method did not adequately describe this weak van der Waals interaction. Both the MP2 and B3LYP geometry optimizations were followed by frequency calculations at the same levels of theory. All geometry optimizations and frequency calculations were carried out with the Gaussian03[46] program.

At the optimized geometries, the standard counterpoise (CP) correction[47] was applied to the binding energies in order to correct for basis set superposition error (BSSE). The counterpoise corrected interaction energies, designated ΔE_{CP}, were calculated as follows

$$\Delta E_{CP} = E^*(\text{complex})_{ab...n} - E^*(\text{A})_{ab...n} - E^*(\text{B})_{ab...n} ... - E^*(\text{N})_{ab...n} \quad (5)$$

where the subscripts denote which 1-particle basis functions were utilized, and the asterisk indicates that the geometry of the complex was used. A deformation energy was also included to account for the geometrical distortion of the monomers from their equilibrium structures in the formation of the complex. These deformation corrections were calculated as the difference in energy between each monomer at its equilibrium geometry and its geometry in the complex, using only the monomer basis sets, that is,

$$\Delta E(\text{N})_{DEF} = E^*(\text{N})_n - E(\text{N})_n \quad (6)$$

for monomer N. The binding energy was then obtained by subtracting the deformation energy of each monomer from the counterpoise corrected interaction energy of eq 5.

$$\Delta E_{BE} = \Delta E_{CP} - \Delta E(\text{A})_{DEF} - \Delta E(\text{B})_{DEF} ... - \Delta E(\text{N})_{DEF} \quad (7)$$

The B3LYP counterpoise corrections and deformation energy calculations were carried out with Gaussian03, whereas the MP2 values were calculated with the MOLPRO[48] suite of ab initio programs. For the open shell molecules, the restricted open shell Hartree−Fock (ROHF) method was used to determine the reference wave functions, and the restricted MP2 (RMP2) method was used to compute the correlation energy contributions. The zero point vibrational energy corrections to the binding energies, denoted ΔE_{ZPE}, were calculated from one-half the sums of the harmonic vibrational frequencies calculated at the same levels of theory as those of the geometry optimizations.

In each case, a correction was included to account for basis set incompleteness. To this end, ΔE_{CP} was computed at the MP2/aVTZ and MP2/aVQZ levels of theory using the MP2/aVDZ geometries. The three MP2 ΔE_{CP} interaction energies (aVDZ, aVTZ, and aVQZ) were then extrapolated with a mixed Gaussian exponential formula:[49,50]

$$\Delta E_{CP}(n) = \Delta E_{CP}(CBS) + f_1 e^{-(n-1)} + f_2 e^{-(n-1)^2} \quad (8)$$

to obtain an estimate of the MP2 complete basis set (CBS) limit. In eq 8, n is the basis set cardinal number (i.e, 2 for DZ, 3 for TZ...), whereas f_1 and f_2 are fitting parameters. For the four open shell complexes $HgX-(H_2O)_3$ and $X-(H_2O)_3$ (X = Cl, Br), MP2/aVQZ calculations were not carried out. For these complexes, ΔE_{CP}(CBS) was estimated using the following formula[51,52]

$$\Delta E_{CP}(CBS) = \Delta E_{CP}(TZ) + \alpha[\Delta E_{CP}(TZ) - \Delta E_{CP}(DZ)] \quad (9)$$

where the scale factor α is given by

$$\alpha = [\Delta E_{CP}(CBS) - \Delta E_{CP}(TZ)]/[\Delta E_{CP}(TZ) - \Delta E_{CP}(DZ)] \quad (10)$$

and was calculated using the $HgX-(H_2O)_2$ and $X-(H_2O)_2$ complexes.

An additional correction to the MP2 ΔE_{CP} was also included to estimate the effects of higher order electron correlation. In these calculations, the coupled cluster singles and doubles method with a perturbative estimate of connected triple excitations [CCSD(T)][53−55] was used to determine ΔE_{CP} using the aVDZ basis sets at the MP2/aVDZ optimized geometries. For the open shell species, the R/UCCSD(T)[55−57] method was used, that is, reference wave functions were determined from ROHF calculations, but the spin restriction was relaxed in the coupled cluster calculations. The correlation correction ΔE_{CC} was then defined as the difference between the ΔE_{CP} values calculated at the CCSD(T)/aVDZ and MP2/aVDZ levels of theory.[58,59]

It should be noted that geometry optimizations and frequency calculations were not carried out using the larger basis sets or with the CCSD(T) method. Therefore, the MP2/aVDZ $\Delta E(\text{N})_{DEF}$ values of eq 6 were used in those cases. The final best estimate binding energies were then obtained as follows:

$$\Delta E_{BE}(\text{best}) = \Delta E_{CP}(\text{CBS}) - \Sigma\Delta E(\text{N})_{DEF} + \Delta E_{CC} \quad (11)$$

III. Results and Discussion

A. Structures. The optimized geometries of $HgBr_2$, HgBr, Br_2, Br atom, and Hg atom with one, two, and three waters are shown in Figures 1−5, respectively. The geometries shown correspond to those optimized at the MP2/aVDZ level of theory. The structures for the other mercury/halogen species not shown in Figures 1−5 are qualitatively similar to those shown and are given in the Supporting Information. Specifically, the optimized geometries of the $HgCl_2$ and HgBrCl complexes closely resemble the structures for $HgBr_2$, with the water molecules in the HgBrCl case preferring configurations where they are more strongly interacting with the Cl atom. The HgCl geometries closely resemble those of HgBr, Cl atom structures resemble those of the Br atom, and the Cl_2 and BrCl cases resemble those of Br_2. The lowest energy BrCl conformers, however, are those in which the water molecules are closest to the Br atom.

In almost every complex, numerous local minima were found on the potential energy surfaces, but only the lowest energy structures are depicted. For many of the complexes, local minima were found that were only tenths of kcal/mol higher in energy than that of the structures shown. This is especially true for the three-water complexes. The $HgBr_2-(H_2O)_3$ complexes pictured in Figures 1c and 6a are excellent examples of this. The conformer pictured in Figure 1c is 0.7 kcal/mol lower in energy than the conformer pictured in Figure 6a when the MP2/aVDZ level of theory was used in the geometry optimizations. However, when the geometries were optimized at the B3LYP/aVDZ level, the relative energetics switch, with the conformer in Figure 6a instead calculated to be 0.7 kcal/mol lower in energy.

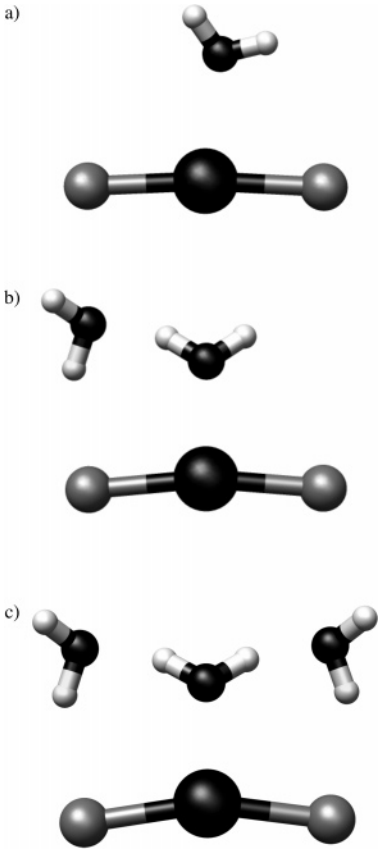

Figure 1. Optimized MP2/aVDZ geometries for $HgBr_2$ with (a) one, (b) two, and (c) three water molecules.

For the most part, however, both the B3LYP and MP2 levels of theory predicted the same conformers to be global minima, which is similar to previous results published on pure water clusters; for example, see ref 60.

There have been a number of previous theoretical and experimental investigations in which the structures of some of the complexes considered in this study have been reported. Soldán et al.[26] optimized the geometry of the Hg−H_2O complex with a variety of methods and basis sets. Their largest basis set, (10s8p7d4f), was used with a relativistic small-core ECP, and the geometry optimizations were carried out with B3LYP, MP2, and quadratic configuration interaction with single and double excitations (QCISD). The current results are in good qualitative agreement with their larger basis set calculations. Both studies found the C_s symmetry conformer shown in Figure 4a to be the global minimum. The MP2/aVDZ Hg−H bond length of the current study was calculated to be 2.81 Å, which is slightly longer than the result of 2.77 Å of Soldán et al. Similarly, the B3LYP Hg−H bond length of the current study was found to be 3.12 Å and is also longer than their B3LYP value of 3.01 Å. In addition, their QCISD bond length of 3.02 Å suggests that MP2 slightly underestimates this quantity. Of course, the structures of the present work could be improved by using larger basis sets and increased levels of electron correlation, but these calculations are outside the scope of this study.

Sevilla et al.[29] have previously reported MP2 structures using small double-ζ basis sets for Cl−H_2O and Cl−$(H_2O)_3$. Roeselová and co-workers[27,28] have reported studies involving Cl−H_2O and Br−H_2O using the Fock space coupled cluster singles and doubles method (FSCC) with double-ζ basis sets. In the case of the single water molecule complexes, the previous calculations and the current results predict a minimum with C_S symmetry, whereby the oxygen of the water is directed toward the halogen atom. This structure is shown in Figure 4a for Br−H_2O. The FSCC method yielded a Br−O bond length of 2.8 Å,[28] which is identical within their reported precision to the

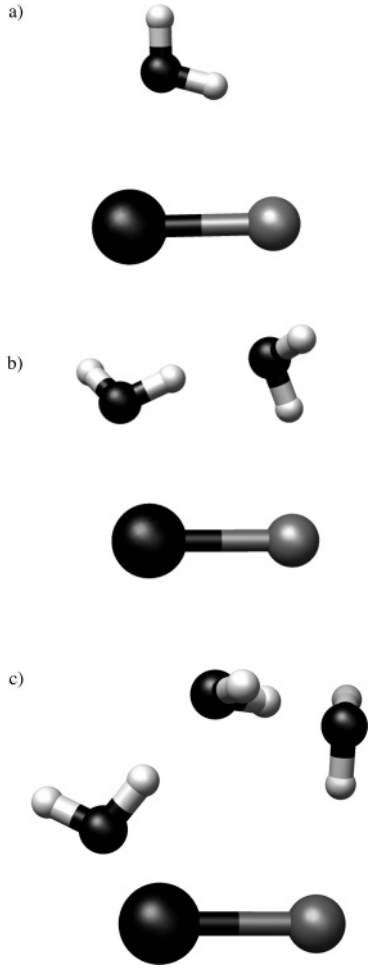

Figure 2. Optimized MP2/aVDZ geometries for HgBr with (a) one, (b) two, and (c) three water molecules.

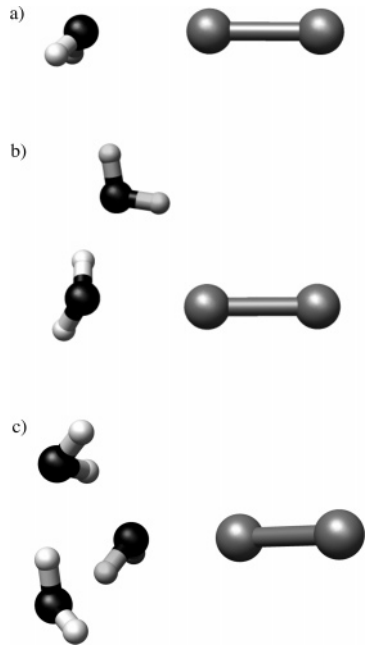

Figure 3. Optimized MP2/aVDZ geometries for Br_2 with (a) one, (b) two, and (c) three water molecules.

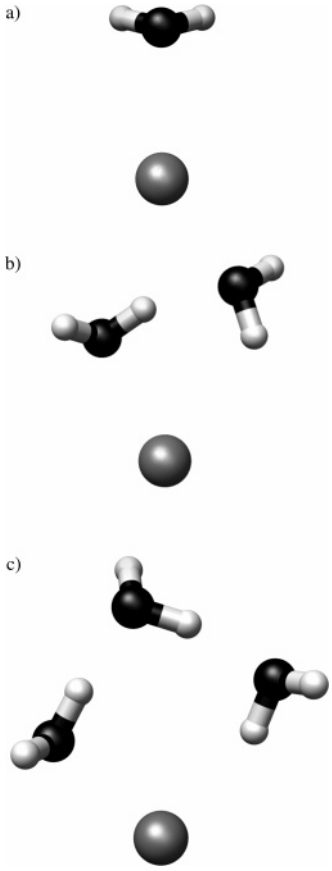

Figure 4. Optimized MP2/aVDZ geometries for the Br atom with (a) one, (b) two, and (c) three water molecules.

current MP2 value of 2.80 Å. The MP2 Cl−O bond length in Cl−H_2O from ref 29 was reported to be 2.70 Å, whereas the FSCC calculations yielded a value of 2.65 Å,[27] both of which agree well with the current MP2 result of 2.70 Å. The present MP2 Cl-O−H_1-H_2 dihedral angle of 109° is also in qualitative agreement with the FSCC value,[27] 105°. The optimized structure in the present work for the Cl−$(H_2O)_3$ complex did not correspond to the same conformer that had been reported previously in ref 29, and this latter conformer is shown in Figure 6b. The conformer pictured in Figure 4c was calculated to be 2.3 kcal/mol lower in energy than that of the confomer in Figure 6b when both were optimized at the MP2/aVDZ level of theory.

The complexes of Br_2, Cl_2, and BrCl with a single water molecule have been previously studied by both experiment and theory. Both the previous studies[32,34−37] and present results indicate that the equilibrium geometries have C_s symmetry with the oxygen atom lying nearly on the X−X bond axis with an obtuse X−O−H−H dihedral angle. The optimized structure of Br_2−H_2O from this work is shown in Figure 3a. The experimental X−O bond lengths of Legon and co-workers[35,37] for Cl_2−H_2O and Br_2−H_2O were determined by pure rotational spectroscopy and reported as 2.848 and 2.851 Å, respectively. The present MP2/aVDZ values of 2.755 and 2.759 Å are shorter by about 0.09 Å. Previously reported ab initio structures[32,34−37] for Br_2 and Cl_2 complexed with a single water molecule were determined using levels of theory similar to that of the present study, that is, either the MP2 or MP3 method with approximately double- or triple-ζ quality basis sets. Thus not suprisingly these are in good qualitative agreement with the structures calculated here. The Br−O bond length in BrCl−H_2O has not been determined experimentally, but the MP2/aug-cc-pVDZ value of Davey and Legon[36] of 2.72 Å is only slightly longer than

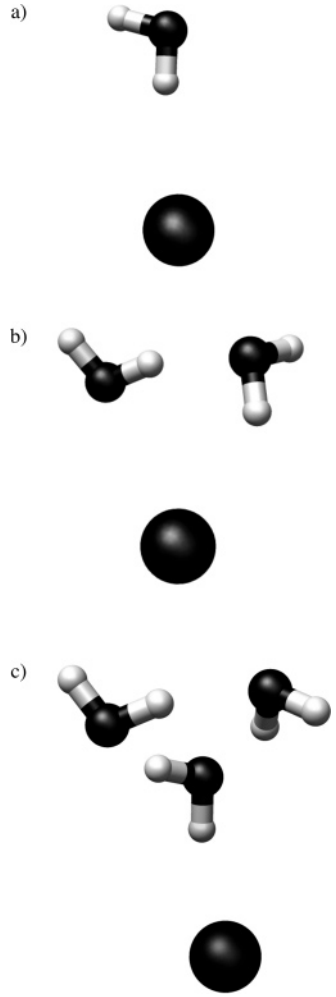

Figure 5. Optimized MP2/aVDZ geometries for the Hg atom with (a) one, (b) two, and (c) three water molecules.

the present value of 2.68 Å. The difference between the present MP2 result and that of ref 36 is likely due to the inclusion of scalar relativistic effects via the PPs in the present work.

There has been one previous report of a multiwater−dihalogen complex, and this was for Br_2 with up to seven water molecules.[34] As part of this study, the authors optimized a conformer of Br_2−$(H_2O)_2$ at the MP2/6-311+G(d,p) level of theory in which the two water molecules were interacting with Br_2 in a relatively independent manner. This structure is shown in Figure 6c. At the MP2/aVDZ level of theory, however, this conformer was found to lie 5.1 kcal/mol above the one pictured in Figure 3b, in which the water molecules are interacting with each other together with the Br_2 molecule.

Other than the conformers just discussed, it appears that structures for the other complexes included in the present study have not been reported previously. With regards to the isolated monomer species, the best estimates of the gas-phase structures of the mercury halide species should be taken from previous ab initio calculations [HgBr, HgCl (ref 25); $HgBr_2$, $HgCl_2$, and HgBrCl (ref 20)], whereas there exist high resolution experimental data for the bond lengths of the dihalogens.[61−64] As shown in Figure 1a−c, addition of water slightly distorts the mercury dihalide molecule from linearity. In addition, as expected, the water interacts most strongly by directing its lone pairs toward the oxidized mercury atom. The mercury halide structures shown in Figure 2a−c also follow this trend with multiple waters forming typical hydrogen-bonding networks.

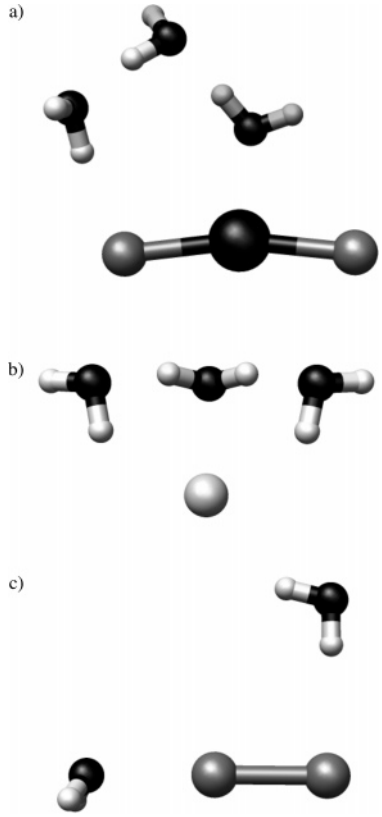

Figure 6. Low-lying alternative conformers for (a) $HgBr_2(H_2O)_3$, (b) $Cl(H_2O)_3$ and (c) $Br_2(H_2O)_2$.

TABLE 1: Equilibrium Incremental Binding Energies (D_e) for HgXY + nH_2O (kcal/mol)

species	theory	basis set	$n=1$	$n=2$	$n=3$
$HgBr_2$	B3LYP	aVDZ	4.18	6.98	9.60
	CCSD(T)	aVDZ	5.00	8.04	7.32
	MP2	aVDZ	5.49	8.44	7.68
		aVTZ	6.16	9.54	8.76
		aVQZ	6.71	10.06	9.27
		CBS	7.06	10.38	9.58
	best estimate[a]		6.57	9.97	9.22
			(5.45)	(7.34)	(7.57)
HgBrCl	B3LYP	aVDZ	4.58	8.97	8.25
	CCSD(T)	aVDZ	5.39	8.53	7.18
	MP2	aVDZ	5.89	8.96	7.52
		aVTZ	6.59	10.01	8.61
		aVQZ	7.14	10.53	9.13
		CBS	7.49	10.85	9.44
	best estimate[a]		6.99	10.42	9.10
			(5.76)	(7.83)	(7.55)
$HgCl_2$	B3LYP	aVDZ	4.81	8.87	8.35
	CCSD(T)	aVDZ	5.56	8.51	7.72
	MP2	aVDZ	6.06	8.92	8.09
		aVTZ	6.73	9.98	9.15
		aVQZ	6.89	10.88	9.68
		CBS	6.98	11.45	10.00
	best estimate[a]		6.47	11.03	9.63
			(5.30)	(8.41)	(8.08)

[a] MP2/CBS + [CCSD(T)/aVDZ − MP2/aVDZ]. The zero-point-corrected values (D_0) are given in parentheses.

B. Incremental Binding Energies. The incremental binding energies are shown in Tables 1−4, with the HgXY complexes contained in Table 1, the HgX and XY complexes contained in Tables 2 and 3, and the atom−water complexes contained in Table 4. As described in section II, the B3LYP binding energies include ΔE_{CP}, $\Delta E(N)_{DEF}$, and ΔE_{ZPE}, all calculated at the B3LYP/aVDZ level of theory. Similarly, the MP2/aVDZ binding energies include the same quantities but calculated at the MP2 level of theory. The CCSD(T)/aVDZ and MP2/CBS limit values, however, utilized the MP2/aVDZ results for $\Delta E(N)_{DEF}$ and ΔE_{ZPE}. Finally, the best estimates of the binding energies shown in these tables are defined as the MP2/CBS binding energy plus the difference between the MP2/aVDZ and CCSD(T)/aVDZ ΔE_{CP} values.

TABLE 2: Equilibrium Incremental Binding Energies (D_e) for HgX + nH_2O (kcal/mol)

species	method	basis	$n=1$	$n=2$	$n=3$
HgBr	B3LYP	aVDZ	3.42	9.30	8.40
	CCSD(T)	aVDZ	3.83	8.11	7.22
	MP2	aVDZ	4.44	9.06	7.59
		aVTZ	5.13	9.95	8.35
		aVQZ	5.55	10.52	
		CBS	5.82	10.87	9.12
	best estimate[a]		5.21	9.92	8.75
			(4.10)	(7.29)	(6.28)
HgCl	B3LYP	aVDZ	4.14	9.98	8.60
	CCSD(T)	aVDZ	4.49	8.69	7.42
	MP2	aVDZ	5.35	9.65	7.73
		aVTZ	6.08	10.64	8.51
		aVQZ	6.57	11.20	
		CBS	6.87	11.55	9.27
	best estimate[a]		6.01	10.59	8.96
			(4.68)	(8.02)	(7.06)

[a] MP2/CBS + [CCSD(T)/aVDZ − MP2/aVDZ]. The zero-point-corrected values (D_0) are given in parentheses.

TABLE 3: Equilibrium Incremental Binding Energies (D_e) for XY + nH_2O (kcal/mol)

species	method	basis	$n=1$	$n=2$	$n=3$
Br_2	B3LYP	aVDZ	3.89	6.81	7.69
	CCSD(T)	aVDZ	3.32	5.96	8.10
	MP2	aVDZ	3.82	6.31	8.19
		aVTZ	4.00	7.05	8.93
		aVQZ	4.26	7.42	9.20
		CBS	4.42	7.65	9.36
	best estimate[a]		3.92	7.30	9.27
			(2.92)	(4.97)	(6.59)
BrCl	B3LYP	aVDZ	5.06	7.24	7.50
	CCSD(T)	aVDZ	4.12	6.19	7.98
	MP2	aVDZ	4.76	6.62	8.05
		aVTZ	5.00	7.40	8.77
		aVQZ	5.31	7.79	9.03
		CBS	5.51	8.03	9.18
	best estimate[a]		4.87	7.60	9.11
			(4.06)	(4.90)	(6.48)
Cl_2	B3LYP	aVDZ	2.71	6.16	8.11
	CCSD(T)	aVDZ	2.47	5.55	8.44
	MP2	aVDZ	2.81	5.78	8.57
		aVTZ	2.96	6.41	9.37
		aVQZ	3.07	6.83	9.65
		CBS	3.14	7.10	9.81
	best estimate[a]		2.80	6.87	9.68
			(2.11)	(4.34)	(6.94)

[a] MP2/CBS + [CCSD(T)/aVDZ − MP2/aVDZ]. The zero-point-corrected values (D_0) are given in parentheses.

A few trends in the binding energies are apparent from Tables 1−4. With the exception of the $Br-(H_2O)_n$ and $Cl-(H_2O)_n$ complexes, all of the MP2/aVDZ binding energies are larger than the CCSD(T)/aVDZ values. The MP2 results are typically about 0.5 kcal/mol higher in energy, but for the HgBr and HgCl complexes, they can be nearly 1 kcal/mol higher than that of their CCSD(T) counterparts. The MP2/CBS binding energies in all cases represent an increase with respect to the MP2/aVDZ values. The differences between the MP2/CBS and aVDZ results are generally larger than the CCSD(T) corrections, with values

TABLE 4: Equilibrium Incremental Binding Energies (D_e) for Atoms + nH_2O (kcal/mol)

species	theory	basis set	$n=1$	$n=2$	$n=3$
Hg	B3LYP	aVDZ			
	CCSD(T)	aVDZ	0.19	4.83	8.41
	MP2	aVDZ	0.59	5.17	8.40
		aVTZ	0.85	5.62	9.53
		aVQZ	0.97	5.93	9.83
		CBS	1.04	6.12	10.00
	best estimate[a]		0.64	5.78	10.00
			(0.29)	(3.70)	(6.93)
Br	B3LYP	aVDZ	5.06	7.90	9.36
	CCSD(T)	aVDZ	2.66	6.38	7.97
	MP2	aVDZ	2.47	6.38	8.08
		aVTZ	2.73	7.08	9.15
		aVQZ	3.01	7.47	
		CBS	3.19	7.72	10.38
	best estimate[a]		3.38	7.72	10.27
			(2.65)	(5.28)	(7.67)
Cl	B3LYP	aVDZ	6.46	8.47	9.72
	CCSD(T)	aVDZ	2.56	6.63	8.00
	MP2	aVDZ	2.34	6.26	8.09
		aVTZ	2.59	7.18	9.24
		aVQZ	2.89	7.60	
		CBS	3.09	7.85	10.42
	best estimate[a]		3.32	8.23	10.33
			(2.68)	(5.51)	(7.64)

[a] MP2/CBS + [CCSD(T)/aVDZ − MP2/aVDZ]. The zero-point-corrected values (D_0) are given in parentheses.

between 1 and 2 kcal/mol. The largest basis set effect is exhibited by the $HgBrCl-(H_2O)_2$ complex, where the MP2/CBS binding energy is larger than the aVDZ value by 2.5 kcal/mol.

It is likely that the best estimates given in Tables 1−4 underestimate the actual binding energies. The CCSD(T) ΔE_{CP} interaction energies were not computed at the CCSD(T) minimum geometry and are thus probably somewhat too small. Since the MP2 ΔE_{CP} values are larger than the CCSD(T) results, the CCSD(T) correction will be too negative. This will therefore likely lead to an underestimation of the actual binding energy. To help quantify this error, CCSD(T)/aVDZ optimizations have been carried out for $HgBr_2$, HgBr, and Br_2 with one water molecule. The ΔE_{CP} values calculated at these CCSD(T) geometries are 0.4, 0.2, and 0.1 kcal/mol larger than those calculated at the MP2 geometries.

There does not appear to be any systematic relationship between the B3LYP/aVDZ binding energies and those computed with MP2/aVDZ or CCSD(T)/aVDZ. However, for the most, part all three methods agree to within ∼1.5 kcal/mol or better. The two exceptions to this trend are the Cl and Br complexes, where the B3LYP binding energies are significantly higher (1.5−3.5 kcal/mol) than those of the other two methods.

The $Hg-H_2O$ binding energies of the current study are in excellent agreement with the previous calculations of Soldán et al.[26] They reported binding energies without a ZPE correction of 0.92 kcal/mol from MP2 calculations and 0.61 kcal/mol using the CCSD(T) method, both employing a large (11s10p8d5f4g) basis set on Hg and aug-cc-pVQZ basis sets on H and O. The current D_e values shown in Table 4, 1.04 kcal/mol with MP2/CBS and a best estimate of 0.64 kcal/mol, agree very well with the values of Soldán et al.

There have also been previous calculations on the binding energies of Br_2, BrCl, and Cl_2 with a single water molecule. In the case of Cl_2-H_2O, Dahl and Røeggen[32] reported a D_e of 2.99 kcal/mol from MP3 calculations using approximately triple-ζ basis sets, whereas Davey et al.[35] determined an MP2/aug-cc-pVDZ D_e of 2.82 kcal/mol. These compare well with the present D_e obtained with MP2/aVDZ of 2.81 kcal/mol. Due to a near cancellation of the CCSD(T) and CBS corrections, all of these values also agree well with the best estimate for D_e of 2.80 kcal/mol. The MP2/aug-cc-pVDZ equilibrium binding energy for $BrCl-H_2O$ was previously calculated to be 4.45 kcal/mol,[36] which is slightly lower, but still very close to the present MP2/aVDZ D_e of 4.76 kcal/mol and the current best estimate of 4.87 kcal/mol. Ramondo et al.[34] conducted ab initio calculations on Br_2-H_2O with the B3LYP and MP2 methods. Their B3LYP/6-311+G(d,p) D_e was calculated to be 4.06 kcal/mol, which is slightly higher than the 3.89 kcal/mol value computed with the B3LYP/aVDZ method in this study (Table 3). Similarly, their MP2/6-311+G(d,p) D_e of 3.59 kcal/mol is in good agreement with the current MP2/aVDZ value of 3.82 kcal/mol. Again, because of a cancellation of basis set effects and higher order electron correlation effects, all values for the D_e of Br_2-H_2O are in good agreement with the present best estimate of 3.92 kcal/mol.

TABLE 5: Effects of Microsolvation on Gas-Phase 0 K Reaction Enthalpies (kcal/mol)[a]

reaction		ΔH_r gas phase[b]	$\Delta\Delta H_r$ $n=1$	$\Delta\Delta H_r$ $n=2$	$\Delta\Delta H_r$ $n=3$
atom−atom recombination					
$Hg + Br \rightarrow$	HgBr	−16.3	−1.5	−3.5	−2.1
$Hg + Cl \rightarrow$	HgCl	−22.9	−2.0	−4.5	−4.0
atom−diatom recombination					
$HgBr + Br \rightarrow$	$HgBr_2$	−73.0	−1.4	−1.4	−2.7
$HgBr + Cl \rightarrow$	HgBrCl	−81.8	−1.7	−2.2	−3.5
$HgCl + Br \rightarrow$	HgBrCl	−75.0	−1.1	−0.9	−1.4
$HgCl + Cl \rightarrow$	$HgCl_2$	−83.8	−0.6	−1.0	−2.0
abstraction					
$HgBr + Br \rightarrow$	$Hg + Br_2$	−30.6	1.2	3.5	3.2
$HgBr + Cl \rightarrow$	Hg + BrCl	−36.5	0.0	2.4	2.2
$HgCl + Br \rightarrow$	Hg + BrCl	−29.7	0.6	3.7	4.3
$HgCl + Cl \rightarrow$	$Hg + Cl_2$	−35.1	2.6	6.3	6.4
insertion					
$Hg + Br_2 \rightarrow$	$HgBr_2$	−42.4	−2.5	−4.9	−5.9
$Hg + BrCl \rightarrow$	HgBrCl	−45.3	−1.7	−4.6	−5.7
$Hg + Cl_2 \rightarrow$	$HgCl_2$	−48.7	−3.2	−7.3	−8.4

[a] n designates the number of water molecules present. [b] Gas phase atom−atom recombination enthalpies were taken from ref 25 with other enthalpies taken from ref 19.

C. Effects of Microsolvation on Reaction Enthalpies. Table 5 contains the 0 K gas-phase enthalpies for a number of mercury−halogen reactions that were taken from earlier ab initio investigations,[19,25] together with the effects of microsolvation from the present study. The gas-phase enthalpies were computed at the CCSD(T)/CBS level of theory using relativistic PPs on Hg and Br and included corrections for core-valence correlation, spin−orbit coupling, scalar relativity, and the pseudopotential approximation. They are expected to be accurate to within ±1 kcal/mol. The effects on the reaction energetics from including water molecules were determined by including 1, 2, or 3 waters with one of the reactants and one of the products. When there were two species in either the reactants or products, all of the water molecules were kept with the species that had the largest binding energies. The microsolvation effects were then calculated as:

$$\Delta\Delta H_r = D_0(\text{solvated reactant}) - D_0(\text{solvated product}) \quad (12)$$

where the D_0 is the total binding energy for removing all waters. For the two- and three-water complexes, D_0 was obtained by adding the incremental binding energies found in Tables 1−4.

The best estimate binding energies were used in all cases to calculate $\Delta\Delta H_r$.

The atom−atom recombination reactions between Hg and Br or Cl are a likely initiation step in the oxidation of mercury during mercury depletion events (MDEs). The gas-phase recombination of these atoms proceeds without a barrier and is exothermic by 16.3 kcal/mol for HgBr and 22.9 kcal/mol for HgCl.[25] Inclusion of water molecules on the Br or Cl reactants, together with the HgBr or HgCl products, slightly increases the exothermicity of the reactions. A single water molecule yields $\Delta\Delta H_r$ values of −1.5 and −2.0 kcal/mol for HgBr and HgCl, respectively, whereas a second water molecule more than doubles the effects to −3.5 and −4.5 kcal/mol, respectively. This trend does not continue with the addition of a third water, where slightly smaller $\Delta\Delta H_r$ values of −2.1 and −4.0 kcal/mol are calculated, respectively.

It has been proposed that the major species being produced during MDEs are Hg(II) species, and three likely possibilities are $HgBr_2$, HgBrCl, and $HgCl_2$. If the formation of HgBr and HgCl is the first step in the oxidation, then one way to form these Hg(II) species would be the atom−diatom recombination reactions given in Table 5, that is, HgX + Y → XHgY. These reactions are also known to proceed without a barrier[24] and are all strongly exothermic by 73−83 kcal/mol. The addition of water molecules also yields an increase in exothermicity, and with three water molecules, the effects are similar in magnitude to the atom−atom recombination reactions.

A set of reactions that can compete with Hg(II) formation arising from atom−diatom recombination are abstraction reactions, HgX + Y → Hg + XY. As shown in Table 4, these reactions are also exothermic, but at about −30 kcal/mol, they are significantly smaller in magnitude than the enthalpies of the atom−diatom recombination reactions. This series of reactions are actually made *less* exothermic by the inclusion of water molecules, and there is a significant increase in the solvation effect between one and two water molecules. This is due primarily to HgX having more ionic character than the XY species. Thus the presence of water would seem to favor the atom−diatom recombination reactions over the abstraction reactions, yielding an increased production of the Hg(II) species.

The final set of reactions to be considered are insertion processes of the type Hg + XY → XHgY. This single step oxidation of Hg(0) to Hg(II) is exothermic by about 45 kcal/mol for Br_2, BrCl, and Cl_2. These reactions, however, are unlikely to occur directly in the gas phase because of large barriers along the reaction path. Multireference configuration interaction (MRCI) calculations have shown that the Hg + Br_2 → $HgBr_2$ reaction has a barrier of about 27 kcal/mol.[24] As might be expected, the inclusion of water molecules also results in these reactions being more exothermic, and the effects are slightly larger than those of the other series of reactions. Presence of a single water molecule increases exothermicity by 2.5, 1.7, and 3.2 kcal/mol for Br_2, BrCl, and Cl_2, respectively, and a second water molecule more than doubles the effect to 4.9, 4.6, and 7.3 kcal/mol, respectively. Addition of a third water further increases the exothermicity. Since the transition state of this insertion reaction arises from a ionic-covalent curve crossing, it is highly likely that the presence of water will also stabilize the transition state with respect to the reactants. If the stabilization of the transition state is significant, it is possible that these reactions would be sufficiently catalyzed by the presence of ice surfaces and water droplets to play a strong role in tropospheric mercury depletion events.

IV. Conclusions

Ab initio calculations have been carried out to determine the structures and binding energies of one, two, and three water molecules with a series of small mercury- and halogen-containing species ($HgBr_2$, HgBrCl, $HgCl_2$, HgBr, HgCl, Br_2, BrCl, Cl_2, Hg, Br, and Cl). These calculations were undertaken to help understand the effects that water vapor, snow, and ice surfaces may have in reactions between mercury and halogen species, which are likely to play an important role in polar tropospheric mercury depletion events. Geometry optimizations were carried out with both the MP2 and B3LYP methods using double-ζ basis sets augmented with diffuse functions. Additional calculations were performed with a series of larger correlation consistent basis sets to estimate binding energies at the complete basis set limit. A further correction for higher order electron correlation effects was calculated using the CCSD(T) method. The counterpoise correction was applied to all binding energies to account for BSSE.

Theoretical structures and binding energies have been reported previously for Hg and halogen atoms as well as dihalogen molecules with one water molecule and for the halogen atoms with multiple water molecules. For these complexes, the binding energies of this study are believed to be among the most accurate currently available. For the other complexes in this work, this is the first time the structures or binding energies have been reported.

The effects of solvation on four series of reactions have been investigated. The atom−atom abstraction reactions, that is, Hg + X → HgX (X = Br, Cl), which have been proposed as a first step in mercury depletion events, were found to increase in exothermicity because of the presence of water. Likewise, the atom−diatom recombination reactions of the form HgX + Y → XHgY (X, Y = Br, Cl) were also found to increase in exothermicity with the inclusion of water molecules. HgX + Y → Hg + XY abstraction reactions, which may compete with atom−diatom recombination, were found to be less exothermic when water was present. Finally, the insertion reactions Hg + XY → XHgY were found to be significantly more exothermic when microsolvation was included.

Acknowledgment. The partial support of this work by the National Science Foundation (CHE-0111282) is gratefully acknowledged.

Supporting Information Available: Details of the geometric, vibrational, and energetic data for all molecular species is available free of charge via the Internet at http://pubs.acs.org.

References and Notes

(1) Schroeder, W. H.; Munthe, J. *Atmos. Environ.* **1998**, *32*, 809.
(2) Schroeder, W. H.; Anlauf, K. G.; Barrie, L. A.; Lu, J. Y.; Steffen, A.; Schneeberger, D. R.; Berg, T. *Nature* **1998**, *394*, 331.
(3) Lindberg, S. E.; Brooks, S.; Lin, C.-J.; Scott, K. J.; Landis, M. S.; Stevens, R. K.; Goodsite, M.; Richter, A. *Environ. Sci. Technol.* **2002**, *36*, 1245.
(4) Temme, C.; Einax, J. W.; Ebinghaus, R.; Schroeder, W. H. *Environ. Sci. Technol.* **2003**, *37*, 22.
(5) Skov, H.; Christensen, J. H.; Goodsite, M. E.; Heidam, N. Z.; Jensen, B.; Wåhlin, P.; Geernaert, G. *Environ. Sci. Technol.* **2004**, *38*, 2373.
(6) Berg, T.; Bartnicki, J.; Munthe, J.; Lattila, H.; Hrehoruk, J.; Mazur, A. *Atmos. Environ.* **2001**, *35*, 2569.
(7) Barrie, L. A.; Bottenheim, J. W.; Schnell, R. C.; Crutzen, P. J.; Rasmussen, R. A. *Nature* **1988**, *334*, 138.
(8) Le, Bras, G.; Platt, U. *Geophys. Res. Lett.* **1995**, *22*, 599.
(9) Boudries, H.; Bottenheim, J. W. *Geophys. Res. Lett.* **2000**, *27*, 517.
(10) Foster, K. L.; Plastridge, R. A.; Bottenheim, J. W.; Shepson, P. B.; Finlayson-Pitts, B. J.; Spicer, C. W. *Science* **2001**, *291*, 471.

(11) Spicer, C. W.; Plastridge, R. A.; Foster, K. L.; Finlayson-Pitts, B. J.; Bottenheim, J. W.; Grannas, A. M.; Shepson, P. B. *Atmos. Environ.* **2002**, *36*, 2721.
(12) Ariya, P. A.; Dastoor, A. P.; Amyot, M.; Schroeder, W. H.; Barrie, L. A.; Anlauf, K.; Raofie, F.; Ryzhkov, A.; Davignon, D.; Lalonde, J.; Steffen, A. *Tellus, Ser. B* **2004**, *56*, 397.
(13) Lu, J. Y.; Schroeder, W. H.; Barrie, L. A.; Steffen, A.; Welch, H. E.; Martin, K.; Lockhart, L.; Hunt, R. V.; Boila, G.; Richter, A. *Geophys. Res. Lett.* **2001**, *28*, 3219.
(14) Gauchard, P.-A.; Aspmo, K.; Temme, C.; Steffen, A.; Ferrari, C.; Berg, T.; Strom, J.; Kaleschke, L.; Dommergue, A.; Bahlman, E.; Magand, O.; Planchon, F.; Ebinghaus, R.; Banic, C.; Nagorski, S.; Baussand, P.; Boutron, C. *Atmos. Environ.* **2005**, *39*, 7620.
(15) Ariya, P. A.; Khalizov, A. F.; Gidas, A. *J. Phys. Chem.* **2002**, *106*, 7310.
(16) Raofie, F.; Ariya, P. A. *Environ. Sci. Technol.* **2004**, *38*, 4319.
(17) Khalizov, A. F.; Viswanathan, B.; Larregaray, P.; Ariya, P. A. *J. Phys. Chem. A* **2003**, *107*, 6360.
(18) Tossell, J. A. *J. Phys. Chem. A* **2003**, *107*, 7804.
(19) Balabanov, N. B.; Peterson, K. A. *J. Phys. Chem. A* **2003**, *107*, 7465.
(20) Balabanov, N. B.; Peterson, K. A. *J. Chem. Phys.* **2003**, *119*, 12271.
(21) Balabanov, N. B.; Peterson, K. A. *J. Chem. Phys.* **2004**, *120*, 6585.
(22) Calvert, J. G.; Lindberg, S. E. *Atmos. Environ.* **2004**, *38*, 5105.
(23) Goodsite, M. E.; Plane, J. M. C.; Skov, H. *Environ. Sci. Technol.* **2004**, *38*, 1772.
(24) Balabanov, N. B.; Shepler, B. C.; Peterson, K. A. *J. Phys. Chem. A* **2005**, *109*, 8765.
(25) Shepler, B. C.; Balabanov, N. B.; Peterson, K. A. *J. Phys. Chem. A* **2005**, *109*, 10363.
(26) Soldan, P.; Lee, E. P. F.; Wright, T. G. *J. Phys. Chem. A* **2002**, *106*, 8619.
(27) Roeselova, M.; Jacoby, G.; Kaldor, U.; Jungwirth, P. *Chem. Phys. Lett.* **1998**, *293*, 309.
(28) Roeselova, M.; Kaldor, U.; Jungwirth, P. *J. Phys. Chem. A* **2000**, *104*, 6523.
(29) Sevilla, M. D.; Summerfield, S.; Eliezer, I.; Rak, J.; Symons, M. C. R. *J. Phys. Chem. A* **1997**, *101*, 2910.
(30) Engdahl, A.; Nelander, B. *J. Chem. Phys.* **1986**, *84*, 1981.
(31) Johnsson, K.; Engdahl, A.; Ouis, P.; Nelander, B. *J. Phys. Chem.* **1992**, *96*, 5778.
(32) Dahl, T.; Røeggen, I. *J. Am Chem. Soc.* **1996**, *118*, 4152.
(33) Liu, Z. F.; Siu, C. K.; Tse, J. S. *Chem. Phys. Lett.* **1999**, *311*, 93.
(34) Ramondo, F.; Sodeau, J. R.; Roddis, T. B.; Williams, N. A. *Phys. Chem. Chem. Phys.* **2000**, *2*, 2309.
(35) Davey, J. B.; Legon, A. C.; Thumwood, J. M. A. *J. Chem. Phys.* **2001**, *114*, 6190.
(36) Davey, J. B.; Legon, A. C. *Phys. Chem. Chem. Phys.* **2001**, *3*, 3006.
(37) Legon, A. C.; Thumwood, J. M. A.; Waclawik, E. R. *Chem.—Eur. J.* **2002**, *8*, 940.
(38) Møller, C.; Plesset, M. S. *Phys. Rev.* **1934**, *46*, 618.
(39) Puzzarini, C.; Peterson, K. A. *Chem. Phys.* **2005**, *311*, 177.
(40) Peterson, K. A.; Figgen, D.; Goll, E.; Stoll, H.; Dolg, M. *J. Chem. Phys.* **2003**, *119*, 11113.
(41) Dunning, T. H., Jr. *J. Chem. Phys.* **1989**, *90*, 1007; Kendall, R. A.; Dunning, T. H., Jr.; Harrison, R. J. *J. Chem. Phys.* **1992**, *96*, 6796.
(42) Woon, D. E.; Dunning, T. H. J. *J. Chem. Phys.* **1993**, *98*, 1358.
(43) Figgen, D.; Rauhut, G.; Dolg, M.; Stoll, H. *Chem. Phys.* **2004**, *311*, 227.
(44) Becke, A. D. *J. Chem. Phys.* **1993**, *98*, 5648.
(45) Stephens, P. J.; Devlin, F. J.; Chabalowski, C. F.; Frisch, M. J. *J. Phys. Chem.* **1994**, *98*, 11623.
(46) Frisch, M. J.; Trucks, G. W.; Schlegel, H. B.; Scuseria, G. E.; Robb, M. A.; Cheeseman, J. R.; Montgomery, J. A., Jr.; Vreven, T.; Kudin, K. N.; Burant, J. C.; Millam, J. M.; Iyengar, S. S.; Tomasi, J.; Barone, V.; Mennucci, B.; Cossi, M.; Scalmani, G.; Rega, N.; Petersson, G. A.; Nakatsuji, H.; Hada, M.; Ehara, M.; Toyota, K.; Fukuda, R.; Hasegawa, J.; Ishida, M.; Nakajima, T.; Honda, Y.; Kitao, O.; Nakai, H.; Klene, M.; Li, X.; Knox, J. E.; Hratchian, H. P.; Cross, J. B.; Bakken, V.; Adamo, C.; Jaramillo, J.; Gomperts, R.; Stratmann, R. E.; Yazyev, O.; Austin, A. J.; Cammi, R.; Pomelli, C.; Ochterski, J. W.; Ayala, P. Y.; Morokuma, K.; Voth, G. A.; Salvador, P.; Dannenberg, J. J.; Zakrzewski, V. G.; Dapprich, S.; Daniels, A. D.; Strain, M. C.; Farkas, O.; Malick, D. K.; Rabuck, A. D.; Raghavachari, K.; Foresman, J. B.; Ortiz, J. V.; Cui, Q.; Baboul, A. G.; Clifford, S.; Cioslowski, J.; Stefanov, B. B.; Liu, G.; Liashenko, A.; Piskorz, P.; Komaromi, I.; Martin, R. L.; Fox, D. J.; Keith, T.; Al-Laham, M. A.; Peng, C. Y.; Nanayakkarra, A.; Challacombe, M.; Gill, P. M. W.; Johnson, B.; Chen, W.; Wong, M. W.; Gonzalez, C.; Pople, J. A.; *Gaussian 03*, revision C.02; Gaussian, Inc.: Wallingford, CT, 2004.
(47) Boys, S. F.; Bernardi, F. *Mol. Phys.* **1970**, *19*, 553.
(48) Amos, R. D.; Bernhardsson, A.; Berning, A.; Celani, P.; Cooper, D. L.; Deegan, A. J.; Dobbyn, A. J.; Eckert, F.; Hampel, C.; Hetzer, G.; Knowles, P. J.; Korona, T.; Lindh, R.; Lloyd, A. W.; McNicholas, S. J.; Manby, F. R.; Meyer, W.; Mura, M. E.; Nicklass, A.; Palmieri, P.; Pitzer, R.; Rauhut, G.; Schütz, M.; Schumann, U.; Stoll, H.; Stone, A. J.; Tarroni, R.; Thorsteinsson, T.; Werner, H.-J. MOLPRO, version 2002.6.
(49) Peterson, K. A.; Woon, D. E.; Dunning, T. H., Jr. *J. Chem. Phys.* **1994**, *100*, 7410.
(50) Feller, D.; Peterson, K. A. *J. Chem. Phys.* **1999**, *110*, 8384.
(51) Peterson, K. A.; McBane, G. C. *J. Chem. Phys.* **2005**, *123*, 084314.
(52) Schwenke, D. W. *J. Chem. Phys.* **2005**, *122*, 014107.
(53) Purvis, G. D. I.; Bartlett, R. J. *J. Chem. Phys.* **1982**, *76*, 1910.
(54) Raghavachari, K.; Trucks, G. W.; Pople, J. A.; Head-Gordon, M. *Chem. Phys. Lett.* **1989**, *156*, 479.
(55) Watts, J. D.; Gauss, J.; Bartlett, R. J. *J. Chem. Phys.* **1993**, *98*, 8718.
(56) Scuseria, G. E. *Chem. Phys. Lett.* **1991**, *176*, 27.
(57) Knowles, P. J.; Hampel, C.; Werner, H.-J. *J. Chem. Phys.* **1994**, *99*, 5219.
(58) Dunning, T. H., Jr.; Peterson, K. A. *J. Chem. Phys.* **2000**, *113*, 7799.
(59) Klopper, W.; Lüthi, H. P. *Mol. Phys.* **1999**, *96*, 559.
(60) Xantheas, S. S. *J. Chem. Phys.* **1995**, *102*, 4505.
(61) Bermejo, D.; Jimenez, J. J.; Martinez, R. Z. *J. Mol. Spectrosc.* **2002**, *212*, 186.
(62) Focsa, C.; Li, H.; Bernath, P. F. *J. Mol. Spectrosc.* **2000**, *200*, 104.
(63) Uehara, H.; Konno, T.; Ozaki, Y.; Horiai, K.; Nakagawa, K.; Johns, J. W. C. *Can. J. Phys.* **1994**, *72*, 1145.
(64) Huber, K. P.; Herzberg, G. *Molecular Spectra and Molecular Structure IV. Constants of Diatomic Molecules*; Van Nostrand: Princeton, NJ, 1979.